CHEMISTRY
A EUROPEAN JOURNAL

DOI: 10.1002/chem.200801506

Electrospray-Ionization Mass Spectrometry for Screening the Specificity and Stability of Single-Stranded-DNA Templated Self-Assemblies

Pim G. A. Janssen, Joost L. J. van Dongen, E. W. Meijer,* and Albertus P. H. J. Schenning*[a]

Abstract: Supramolecular complexes consisting of a single-stranded oligothymine (**dT*n***) as the host template and an array of guest molecules equipped with a complementary diaminotriazine hydrogen-bonding unit have been studied with electrospray-ionization mass spectrometry (ESI-MS). In this hybrid construct, a supramolecular stack of guest molecules is hydrogen bonded to **dT*n***. By changing the hydrogen-bonding motif of the DNA host template or the guest molecules, selective hydrogen bonding was proven. We were able to detect single-stranded-DNA (ssDNA)–guest complexes for strands with lengths of up to 20 bases, in which the highest complex mass detected was 15 kDa; these complexes constitute 20-component self-assembled objects. Gas-phase breakdown experiments on single- and multiple-guest–DNA assemblies gave qualitative information on the fragmentation pathways and the relative complex stabilities. We found that the guest molecules are removed from the template one by one in a highly controlled way. The stabilities of the complexes depend mainly on the molecular weight of the guest molecules, a fact suggesting that the complexes collapse in the gas phase. By mixing two different guests with the ssDNA template, a multicomponent dynamic library can be created. Our results demonstrate that ESI-MS is a powerful tool to analyze supramolecular ssDNA complexes in great detail.

Keywords: mass spectrometry · nucleic acids · self-assembly · supramolecular chemistry · templates

Introduction

DNA is a promising scaffold[1–11] for organizing small molecules through a noncovalent bottom-up approach to create monodisperse nanosized objects.[12–16] Noncovalent approaches such as groove binding,[1–3] intercalation,[1–3] hydrogen bonding,[7–11] and metal–ligand binding[17] have been reported. Furthermore, DNA can, for example, be used as a building block to construct complex nanosized objects through sticky-end cohesion.[18–27] With this approach, DNA polyhedra[25] and gridded structures[26,27] have been constructed. Insight into the strength and dynamics of binding is essential for a deeper understanding of these DNA constructs and will help the exploitation of this approach. DNA constructs are usually analyzed by spectroscopic or microscopic techniques. A technique that is less explored is ESI-MS, which is a soft technique that transfers solutes into the gas phase and allows the study of noncovalent interactions and large nonvolatile chargeable biomolecules such as proteins[28–30] and nucleic acids.[31–38] Furthermore, this technique has recently been used to characterize a variety of supramolecular complexes.[39–45] Qualitative information on the binding strength of the supramolecular complexes can be obtained by collision-induced-dissociation (CID) experiments.[46]

Recently, we have reported the ssDNA-templated self-assembly of naphthalene and oligo(*p*-phenylene)vinylene diaminotriazine derivatives (**G1** and **G4**, respectively) that bind to a complementary strand of oligothymine (**dT40**, in which 40 is the number of thymines) to yield uniform objects (Figure 1 and Scheme 1).[11,47] With ESI-MS, we have been able to detect distinct complexes of **G1** or **G4** with **dT10**.[11] The ESI-MS technique has also been used to study noncovalent double-stranded-DNA (dsDNA)–guest complexes[9,48] to enable drug screening.[49–51] In addition to the probing of selective hydrogen bonds[9] or the binding stoichi-

[a] P. G. A. Janssen, J. L. J. van Dongen, Prof. Dr. E. W. Meijer, Dr. A. P. H. J. Schenning
Laboratory of Macromolecular and Organic Chemistry
Eindhoven University of Technology
P.O. Box 513, 5600 MB Eindhoven (The Netherlands)
Fax: (+31) 40-245-1036
E-mail: e.w.meijer@tue.nl
a.p.h.j.schenning@tue.nl

Supporting information for this article is available on the WWW under http://dx.doi.org/10.1002/chem.200801506.

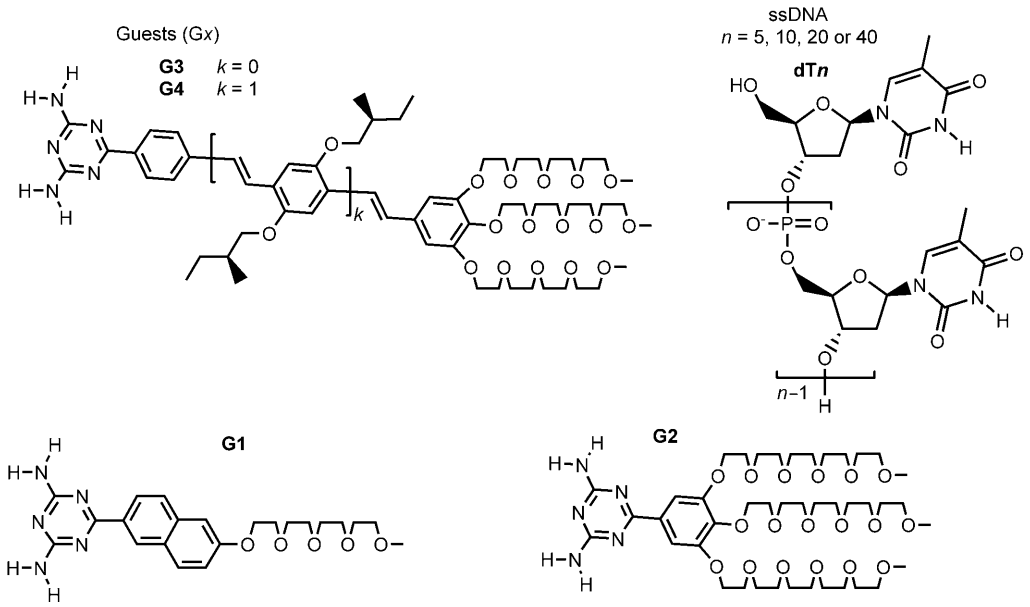

Scheme 1. Molecular structures of **dT*n*** and the guests (**G*x***).

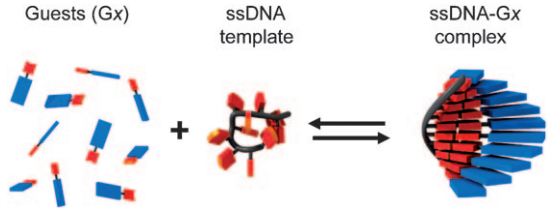

Figure 1. Schematic representation of the formation of the **dT*n***–guest complexes. Blue bars: guests; red bars: hydrogen-bonding motif; black strand: DNA backbone.

ometry, the affinities and selectivities of minor-groove binders[49,50] have been proven with ESI-MS and CID experiments. In the present study, ESI-MS is used to systematically study the effects of template lengths and guest-molecule size on complex detectabilities to explore the scope and limitations of this technique for these supramolecular self-assemblies. With CID experiments, the relative strength of guest binding to the ssDNA template in the gas phase was studied. Finally, ESI-MS was used for combinatorial screening of these hybrid systems, in mixtures of two guests together with the ssDNA template.

Results and Discussion

Detection of ssDNA–guest complexes: First, the supramolecular complexes in ultrapure water with the template **dT10** and different guests, **G*x***, were studied under mild conditions with ESI-MS in the negative mode. We systematically increased the strength of possible π–π interactions in the complexes by using guest derivatives equipped with different diaminotriazine hydrogen-bonding units, from a benzene (in **G2**),[52] to a naphthalene (in **G1**),[11] a stilbene (in **G3**), and finally an oligo(*p*-phenylene)vinylene (in **G4**)[11] core (Figure 1 and Scheme 1). The guests themselves were hardly detectable in the negative mode because the basic diaminotriazine-substituted guests are barely deprotonated under our ESI-MS conditions in ultrapure water.[53] The ESI mass spectra of solutions of **dT10** show peaks for negatively charged single strands $[\mathbf{dT10}]^{z-}$, in which z is the number of charges (Figure 2a). The ESI mass spectra of the solutions containing ten equivalents of **G1** relative to **dT10** show $[\mathbf{dT10}+m\,\mathbf{G1}]$ complex peaks (in which m is the number of **G1** molecules) and the $[\mathbf{dT10}]^{z-}$ peaks; the guests are now also visible as deprotonated guest molecules, $[\mathbf{G1}-\mathrm{H}]^{1-}$ (Figure 2b). Deconvolution of this ESI mass spectrum yields masses of distinct $[\mathbf{dT10}+m\,\mathbf{G1}]$ complexes with up to 11 guests bound; $[\mathbf{dT10}+6\,\mathbf{G1}]$ has the most intense complex peak (Figure 2c).[54] Remarkably, the number of guests bound is larger than the number of binding sites available on the template. The detection of $[\mathbf{dT10}+11\,\mathbf{G1}]$ complex peaks could be caused by further aggregation of the guest molecules to the complex during the formation of nanodroplets.[55] The concentration inside such a droplet quickly increases during the evaporation process[28,29] and can easily reach 1.2 mM, at which point **G1** starts to form aggregates at room temperature.[11] The presence of the $[\mathbf{G1}-\mathrm{H}]^{1-}$ peak suggests that, during the evaporation process and flight of the ions to the detector, the complex can dissociate, which leads to a distribution of distinct complexes that is not necessarily present in solution.

Titration experiments in which up to 20 equivalents of **G1** were added to **dT10** show that, already at 6 equivalents of **G1**, fully covered **dT10**–**G1** complexes are observed (Figure 3). For lower amounts of guest molecules (<6 equiv), the concentration of **G1** is too low for significant

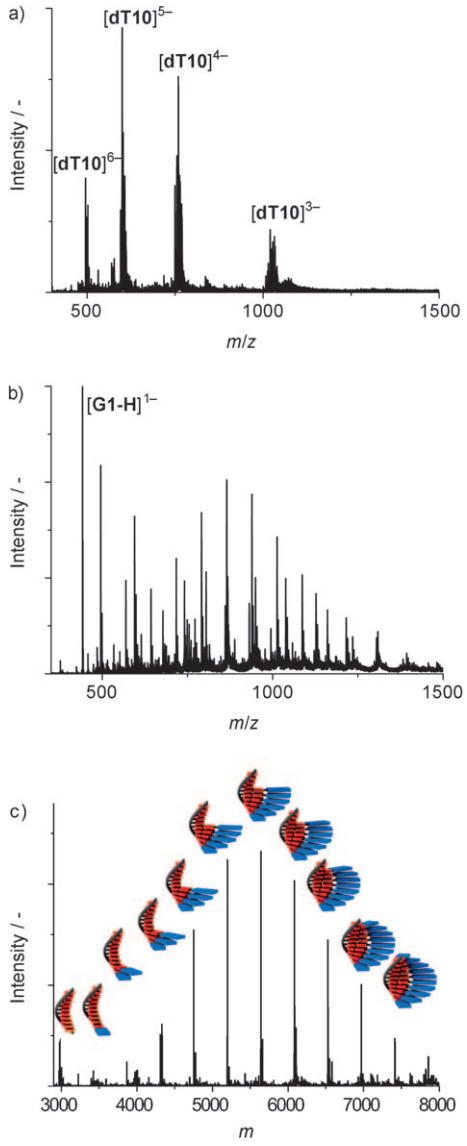

Figure 2. ESI mass spectra for a) [**dT10**] = 0.05 mM and b) [**G1**] = 0.5 mM and [**dT10**] = 0.05 mM in ultrapure water. c) Deconvoluted spectrum for [**G1**] = 0.5 mM and [**dT10**] = 0.05 mM in ultrapure water.

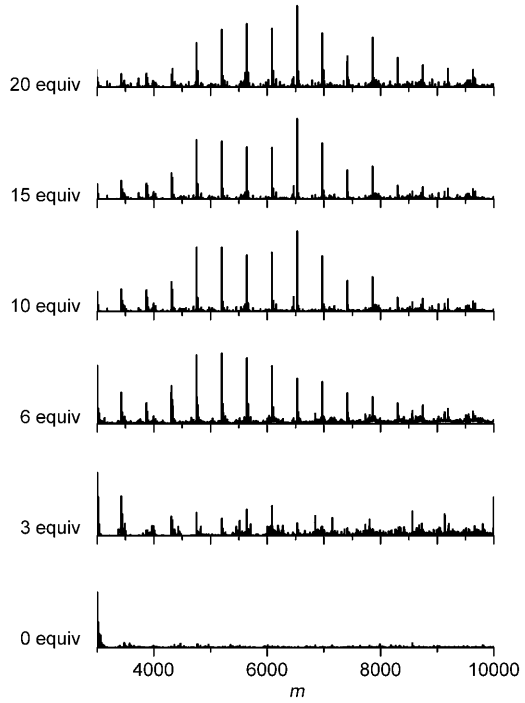

Figure 3. Deconvoluted ESI mass spectra for titration experiments in which [**G1**] is increased from 0 to 0.45 mM and [**dT10**] is kept constant at 0.0225 mM in ultrapure water.

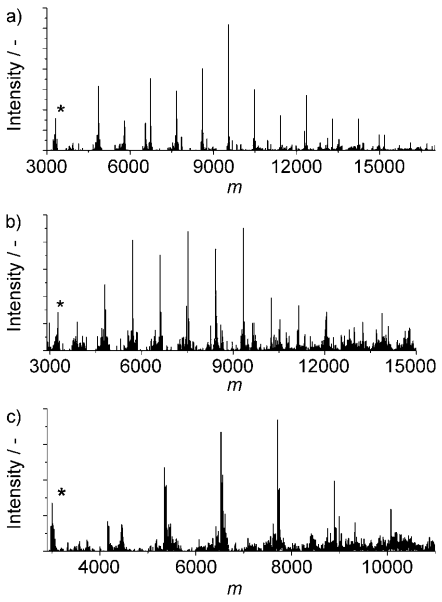

Figure 4. Deconvoluted ESI mass spectra for a) [**G2**] = 1 mM and [**dT10**] = 0.1 mM, b) [**G3**] = 1 mM and [**dT10**] = 0.1 mM, and c) [**G4**] = 0.5 mM and [**dT10**] = 0.05 mM in ultrapure water. * indicates the mass of the molecular ion for **dT10**.

binding, whereas the distribution and intensity of the peaks hardly changes with 10 equivalents or more.[56] With 20 equivalents of guest molecule, the same distribution is present as with 10 and 15 equivalents, which suggests that, at these concentrations of **G1**, most **dT10** templates are fully covered with **G1** in solution.

Other diaminotriazine-equipped guest molecules were also tested for binding to **dT10**. Mixtures containing ten equivalents of the gallic acid derivative **G2**, the stilbene derivative **G3**, or the oligo(*p*-phenylene)vinylene derivative **G4** all showed complex peaks when mixed with **dT10** (Figure 4).[57] For **G2** and **G3**, similar spectral features to those of **G1** were observed, whereas only up to six guests bound to **dT10** have been detected for **G4** complexes.

We also changed the size of the template for **dT*n*/G1** mixtures with $n = 5$, 20, or 40, in which we kept the concentration of **G1** the same and added a base equivalent of the ssDNA template. The solution experiments with these mixtures all showed binding of **G1** to the **dT*n*** template.[58] For **dT5–G1** and **dT20–G1** complexes, the mass spectra could be deconvoluted (Figure 5a and b) and up to 5 and 19 **G1** mol-

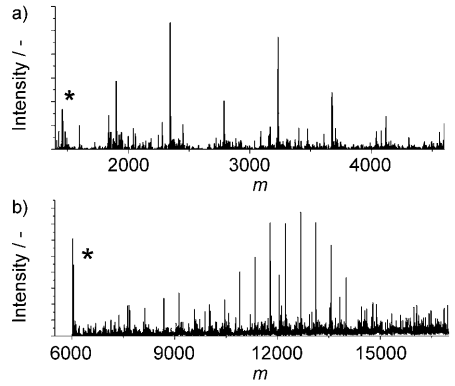

Figure 5. Deconvoluted ESI mass spectra for a) [**G1**] = 1 mM and [**dT5**] = 0.2 mM and b) [**G1**] = 1 mM and [**dT20**] = 0.05 mM in ultrapure water. * indicates the mass of the molecular ions for **dT5** or **dT20**, respectively.

ecules bound to the template, respectively, have been detected.[59] The mass spectrum of the longer **dT40** with **G1** only shows the $[\mathbf{G1}-H]^{1-}$ peak and some **dT40** degradation-product peaks.[47] The $[\mathbf{dT40}]^{z-}$ peaks are not visible, whereas they are visible without guest molecules.[47]

In all of the experiments above, distinct **dT*n*–G** complexes have been detected; these can reach up to a maximum mass of 15 kDa in the case of a ssDNA length of 20 bases. For **dT40**/**G1** mixtures, no distinct complexes have been detected. Still, the presence of the $[\mathbf{G1}-H]^{1-}$ peak and the lack of $[\mathbf{dT40}]^{z-}$ peaks is evidence that **G1** binds to **dT40**.[47,58] The binding of the guest molecules observed with ESI-MS is in agreement with the solution experiments.[11] The reason that no distinct complex peaks are observed for the **dT40–G1** complex could be the relatively lower concentration of complex, the high number of possible peaks, the high molecular weights of the **dT40–G1** complexes (from 12 to 30 kDa) that considerably broaden the peaks, or the purity or fragmentation of **dT40**. The presence of a very small amount of Na^+ and K^+ ions will further increase the number of peaks for each [**dT40**+*m***G1**] complex.

Selectivity study: To see whether the observed binding of the guest to the template is selective, a variety of control experiments were performed. When **G1** is added to the homo-DNA strands **dA5**, **dA10**, **dA20**, **dG10**, or **dC10** (Scheme 2) under the same conditions as those used for **dT*n***, the most intense peaks are from the free ssDNA, and only a few **G1** molecules are bound to the ssDNA templates, which is in line with the solution experiment.[11,58] In titration experiments in which up to 20 equivalents of **G1** were added to **dT10** or **dA10**, the detected amount of free **dA10** is higher than that of free **dT10**.[47] Also, a higher number of **G1** guest molecules bind to **dT10** rather than to **dA10** during the whole titration. The control experiments with other homo-ssDNA strands clearly show that there is a clear preference for binding to **dT10**, which is logical when it is considered that threefold hydrogen bonding is possible for a thymine–**G1** complex.

The methyl ester derivative **G5** (Scheme 2) and adenine (**G6**) did not show binding to **dT10**,[47] whereas up to six adenosines (**G7**), which is more water soluble than adenine, bound to **dT10** have been detected.[47] These experiments reveal that the binding of the diaminotriazine to the template occurs through hydrogen bonding. This conclusion is supported by a competition experiment in which an excess of complementary **dA20** strands is added to the **dT20–G1**

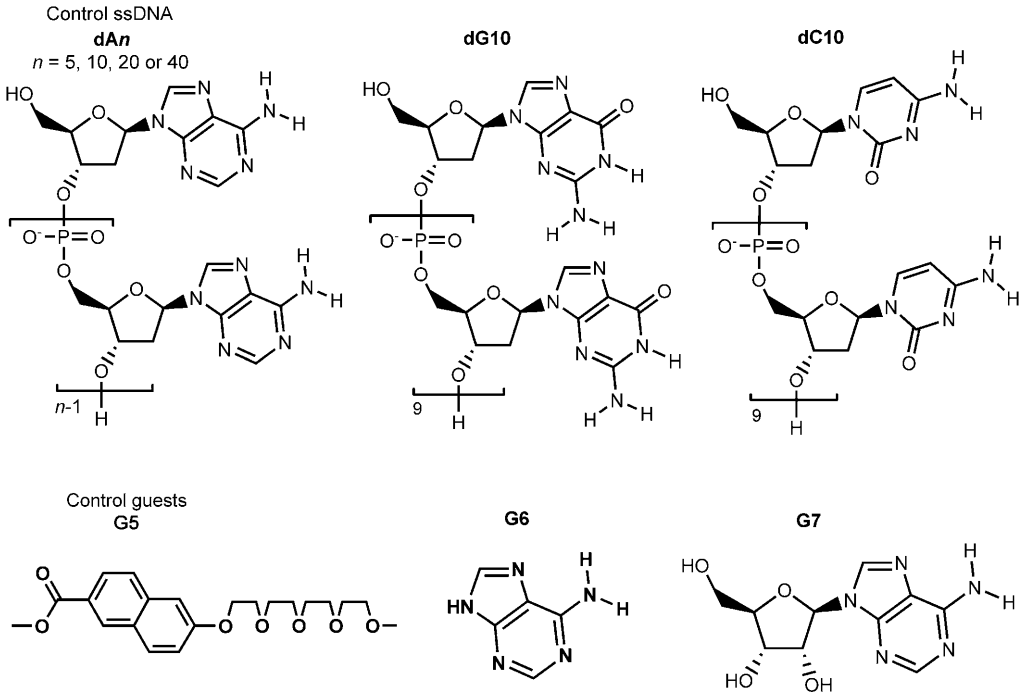

Scheme 2. Molecular structures of the control ssDNA and control guests.

complexes in solution to yield the more stable dsDNA.[47,60] This proves that the diaminotriazine unit binds to the **dT20** template through hydrogen bonding[61] and that the **dT20**–**dA20** double strand is more stable than the **dT20**–**G1** complex. These results agree with the previously reported solution experiments with CD spectroscopy analysis, in which the complementary strand **dA40** (Scheme 2) was added to a mixture containing the **dT40**–**G1** complex.[11]

Collision-induced-dissociation experiments: The relative stability of the ssDNA–guest complexes was studied by CID experiments or tandem mass spectrometry on selected complexes in the gas phase. After sample ionization, a single complex of interest is isolated with the quadrupole mass analyzer and only this isolated complex enters the collision cell, in which the selected ion subsequently collides with the collision gas. The degree of dissociation depends on the mass of the collision gas used, the gas pressure in the collision cell, and the acceleration voltage, V_{acc}, which determines the kinetic energy of the ion. A higher acceleration voltage yields a higher kinetic energy for the complex and, thus, a higher collision energy between the complex and the collision gas, argon in our case. With a higher V_{acc} value or a higher argon pressure in the collision cell, more guest molecules are dissociated, either as neutral or charged species, and this eventually results in virgin ssDNA. The argon pressure in the collision cell was set to 1.2×10^{-3} mbar, at which value each ion faces multiple collisions with the collision gas. We monitored the dissociative pathway and the degree of dissociation of the isolated ion as a function of the voltage in the collision cell.[29,62] Quantitative values for guest-binding energies cannot be obtained with these CID experiments, because the threshold energy of dissociation cannot be determined with our setup. The breakdown curve of a single complex is measured by selecting a narrow m/z range around the m/z value of the complex with the quadrupole and by increasing the V_{acc} value in the collision cell. The mass spectrum then shows the breakdown of the selected complex and the appearance of the breakdown products of the selected complex. The ion-survival yield (%) of the parent ion and the appearance of collision products at each V_{acc} value were calculated relative to the total intensities of all ions detected according to Equation (1), in which $I[\mathbf{dTn}+m\,\mathbf{G}]^{z-}$ is the intensity of the corresponding ion.

$$\text{Appearance } [\mathbf{dTn}+m\,\mathbf{G}]^{z-} = \frac{I[\mathbf{dTn}+m\,\mathbf{G}]^{z-}}{\sum_{m=0}^{n} I[\mathbf{dTn}+m\,\mathbf{G}]^{z-}} \times 100\,\% \tag{1}$$

For a fair comparison between the different complexes, the collision energy, E_{CM}, was corrected for the center of mass according to Equation (2), in which E_{lab} is the kinetic energy of the ion obtained in the accelerator, z is the number of charges, V_{acc} is the acceleration voltage, M_g is the mass of the collision gas (argon), and M_i is the mass of the parent ion.[29]

$$E_{CM} = E_{lab}\frac{M_g}{M_i+M_g} = zV_{acc}\frac{M_g}{M_i+M_g} \tag{2}$$

For the CID experiment, we initially studied $[\mathbf{dT5}+m\,\mathbf{G1}]^{z-}$ complexes because these low-molecular-weight ions had a sufficiently high intensity of the parent ions. The CID ion-appearance plots show that, for up to triply charged complexes, the breakdown occurs through sequential loss of neutral **G1** molecules, as shown, for example, with the $[\mathbf{dT5}+2\,\mathbf{G1}]^{3-}$ complex (Figure 6a). In contrast, the dissociation of the quadruply charged complexes shows

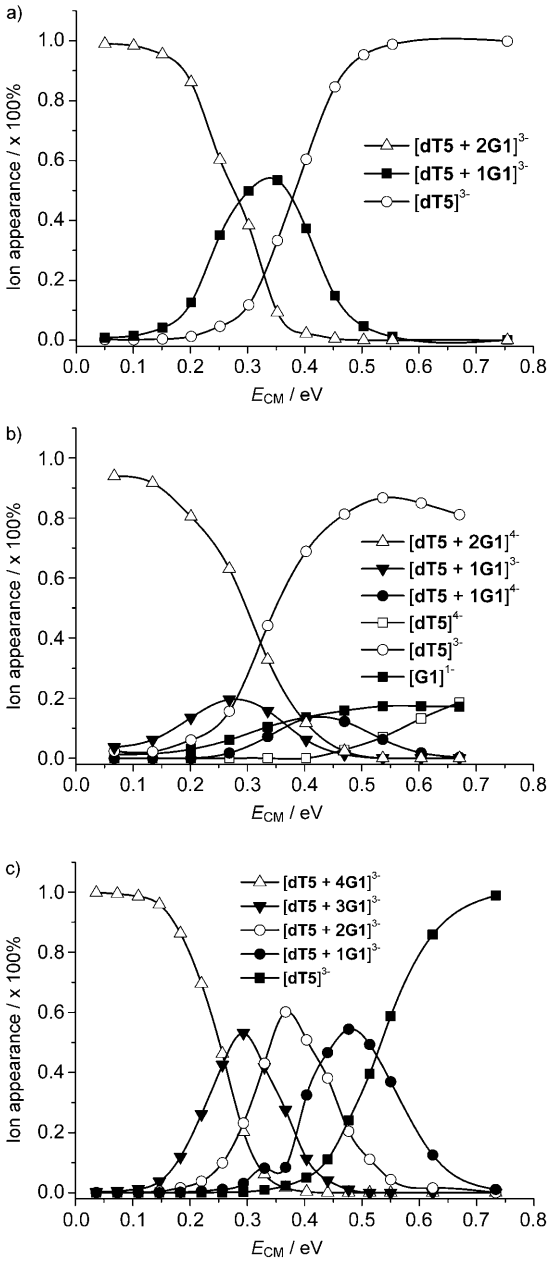

Figure 6. Ion-appearance plots for the CID experiments of a) $[\mathbf{dT5}+2\,\mathbf{G1}]^{3-}$ (m/z 780.92 g mol^{-1}), b) $[\mathbf{dT5}+2\,\mathbf{G1}]^{4-}$ (m/z 585.45 g mol^{-1}), and c) $[\mathbf{dT5}+4\,\mathbf{G1}]^{3-}$ (m/z 807.06 g mol^{-1}) as a function of the collision energy, E_{CM}.

two fragmentation pathways. For instance, for the $[\mathbf{dT5}+2\,\mathbf{G1}]^{4-}$ complex (Figure 6b), neutral **G1** molecules and charged $[\mathbf{G1}-\mathrm{H}]^{1-}$ ions can be dissociated. It is remarkable that, due to the increased charge repulsion,[50] the basic amines of the diaminotriazine are deprotonated. The breakdown of the triply charged complex with four guests, $[\mathbf{dT5}+4\,\mathbf{G1}]^{3-}$, also shows a breakdown mechanism whereby neutral **G1** molecules are sequentially dissociated (Figure 6c). At $E_{CM}=0.2$ eV, which corresponds to a V_{acc} value of 5 V, a very low voltage for ESI-MS experiments, only 90% of the parent ion survives. This implies that, even when all DNA templates are still fully covered after the ionization process, a distribution will always be present in the ESI mass spectrum due to fragmentation in the collision cell at this pressure. The gas-phase stabilities of the parent ions of the $[\mathbf{dT5}+m\,\mathbf{G1}]^{z-}$ complexes as a function of the number of guests, m, and charges, z, were compared through the parent-ion survival yield as a function of the E_{CM} and I_{50} (E_{CM} value at which 50% of the parent ion survives) values (Figure 7). In a comparison of a single, only hydrogen-

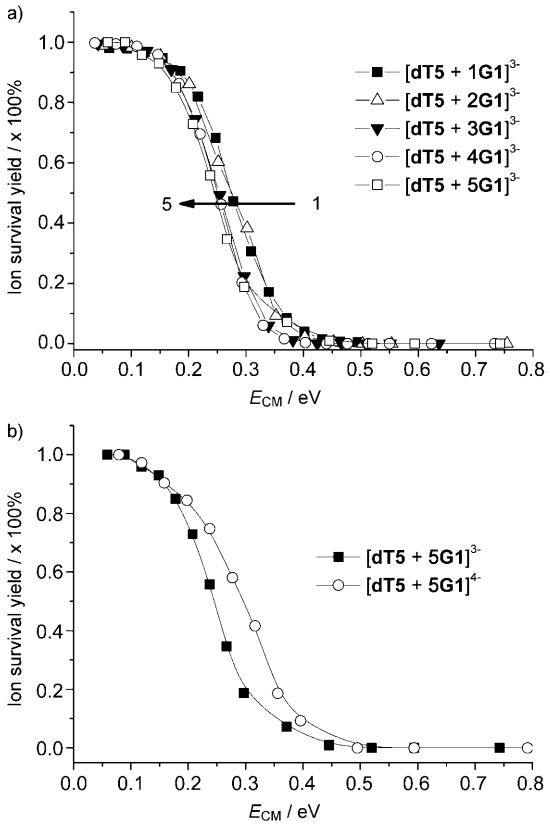

Figure 7. Parent-ion survival yields for the CID experiments of a) $[\mathbf{dT5}+m\,\mathbf{G1}]^{3-}$ and b) $[\mathbf{dT5}+5\,\mathbf{G1}]^{z-}$. The lines are included to guide the eyes.

bonded guest with multiple-bound guests, the I_{50} value when multiple guests are bound should be significantly higher than that when one guest is bound because of additional guest–guest interactions However, clearly, both the m and z values do not change the I_{50} value to a large extent (Figure 7 and Table 1). We found that $I_{50}=0.27$ eV for $[\mathbf{dT5}+1\,\mathbf{G1}]^{3-}$ and $I_{50}=0.25$ eV for $[\mathbf{dT5}+5\,\mathbf{G1}]^{3-}$, that is, a difference of

Table 1. I_{50} values of $[\mathbf{dT5}+m\,\mathbf{G}x]^{z-}$ ions.

Ion	I_{50} value [eV] $m=\mathbf{1}$	$m=\mathbf{2}$	$m=\mathbf{3}$	$m=\mathbf{4}$	$m=\mathbf{5}$
$[\mathbf{dT5}+m\,\mathbf{G1}]^{4-}$	n.d.[a]	0.30	0.30	0.28	0.28
$[\mathbf{dT5}+m\,\mathbf{G1}]^{3-}$	0.27	0.27	0.25	0.25	0.25
$[\mathbf{dT5}+m\,\mathbf{G2}]^{3-}$	0.60	n.d.[a]	0.45	n.d.[a]	n.d.[a]
$[\mathbf{dT5}+m\,\mathbf{G3}]^{3-}$	0.55	n.d.[a]	0.42	n.d.[a]	n.d.[a]
$[\mathbf{dT5}+m\,\mathbf{G4}]^{3-}$	0.70	n.d.[a]	0.62	n.d.[a]	n.d.[a]

[a] n.d. = not determined.

less than 10%. Hence, the dissociation is neither cooperative nor anti-cooperative. Apparently, these complexes do not necessarily retain their solution structure when brought into the gas phase, but collapse into a structure with more host–guest interaction (see below). When compared, the quadruply charged complexes appear to be slightly more stable than the triply charged complexes (Figure 7b); for instance, with five **G1** molecules bound, $I_{50}=0.28$ and 0.25 eV for the quadruply and triply charged complexes, respectively.

To study the relative gas-phase stabilities of the complexes with the different guests, CID experiments were performed on $[\mathbf{dT5}+1\,\mathbf{G}x]^{3-}$ and $[\mathbf{dT5}+3\,\mathbf{G}x]^{3-}$ complexes (Figure 8) under standard conditions. The corresponding ion peaks were selected and the voltage of the collision cell was increased until the parent ions were no longer detected. It should be noted that the E_{CM} value has been corrected for the mass of the parent ion for a fair comparison. When three guests are bound, it is clear that the larger guests bind more strongly, as indicated by the higher I_{50} value (Figure 8a and Table 1). This agrees well with an increased guest–guest interaction for bigger guest molecules. When $[\mathbf{dT5}+3\,\mathbf{G}x]^{3-}$ and $[\mathbf{dT5}+1\,\mathbf{G}x]^{3-}$ are compared, the I_{50} value of $[\mathbf{dT5}+1\,\mathbf{G}x]^{3-}$ is lower in all cases, results that are similar to those already found for **G1** (Figure 8 and Table 1). For $[\mathbf{dT5}+1\,\mathbf{G}x]^{3-}$ individually, no or hardly any difference in the I_{50} value is expected if the guests are only hydrogen bonded to the DNA template. By contrast, for collapsed structures in which the sum of all the van der Waals interactions will count, the I_{50} value should increase with the molecular weight of the guests. Here, we notice an apparent linear increase of the I_{50} value of the $[\mathbf{dT5}+1\,\mathbf{G}x]^{3-}$ parent ions with the molecular weight of the guest molecules (Figure 8 and Table 1). This clearly shows that the templated structures that are present in solution collapse in the gas phase as observed earlier.[30,63,64] This structural collapse can easily occur during the evaporation process or during the several tens of microseconds when the ions travel through the collision cell.[64,65]

Mixed guest systems: We have also performed competition experiments in which two guests are mixed in solution with

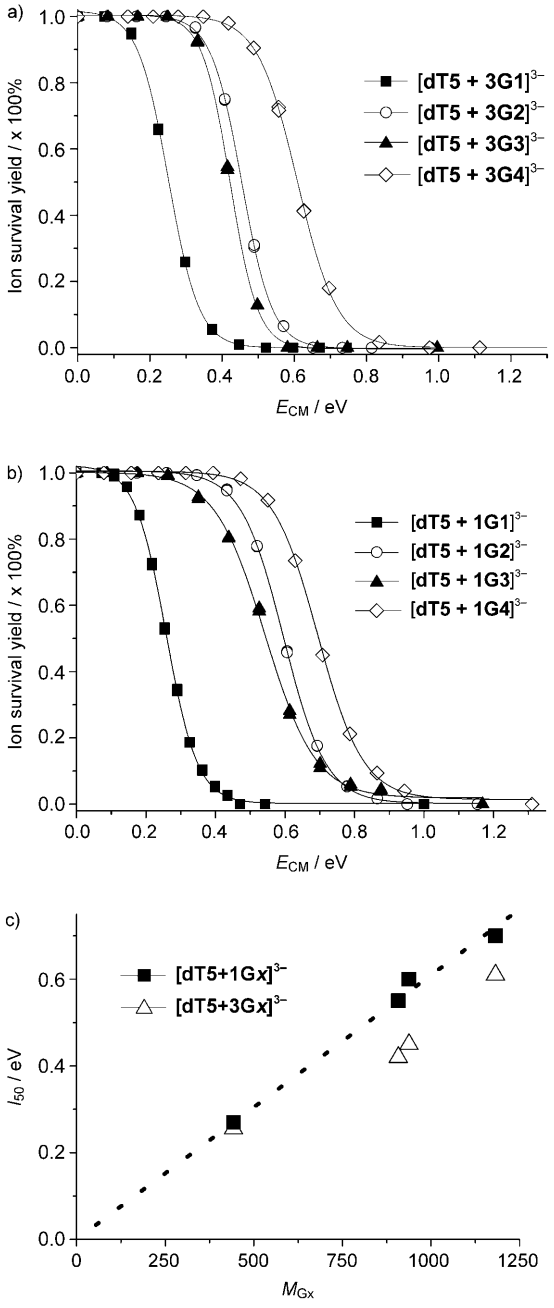

Figure 8. Parent-ion survival yields for the CID experiments of a) $[\mathbf{dT5}+3\mathbf{G1}]^{3-}$ and b) $[\mathbf{dT5}+1\mathbf{G}x]^{3-}$. c) Plot of the I_{50} value of the parent ions versus the mass of the guest molecule. The lines are included to guide the eyes.

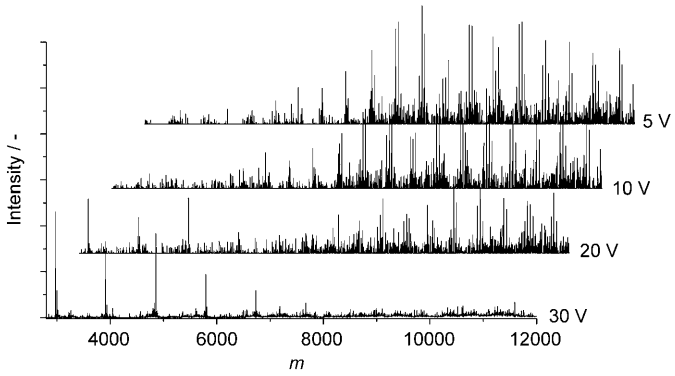

Figure 9. Deconvoluted ESI mass spectra at different V_{acc} values for $[\mathbf{G1}]=[\mathbf{G2}]=1$ mM and $[\mathbf{dT10}]=0.1$ mM.

the **dT10** template and only ions in which **G2** is bound are detected; this shows that **G2** binds more strongly to **dT10** than **G1**. This is in good agreement with the I_{50} values obtained from the CID experiments (Table 1). Mixtures of **dT5** or **dT10** with **G1** and **G3** or **G1** and **G4** showed comparable results, in that **G1** again dissociates prior to **G3** or **G4**.[47]

To determine the relative stability of two different guests, we performed CID experiments on $[\mathbf{dT5}+1\mathbf{G1}+1\mathbf{G}x]^{3-}$ complexes. The results for the $[\mathbf{dT5}+1\mathbf{G1}+1\mathbf{G2}]^{3-}$ complex are shown in Figure 10, which is also representative for the

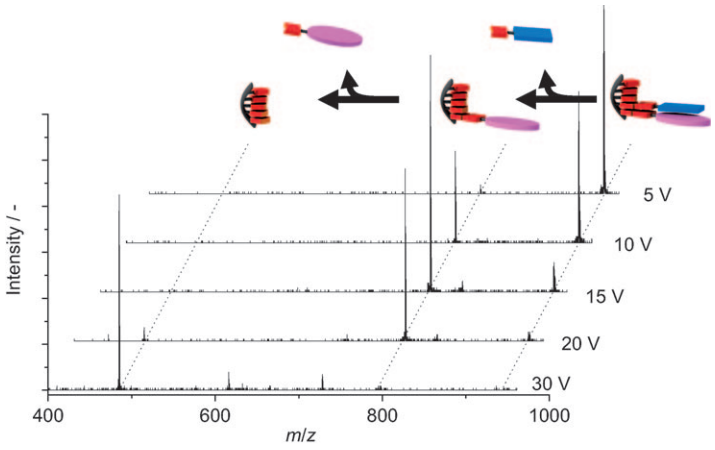

Figure 10. ESI mass spectra of the $[\mathbf{dT5}+1\mathbf{G1}+1\mathbf{G2}]^{3-}$ ion at different V_{acc} values.

the ssDNA template. We added one base equivalent of each guest for a fair competition experiment. As an illustrative example, **G1** was mixed with **G2** in the presence **dT10** (Figure 9).[66] Under mild conditions, with $V_{acc}=15$ V, distinct complexes of **dT10** with both **G1** and **G2** bound in various ratios can be detected with masses of up to 12000 Da. When the V_{acc} value is increased, the ions are broken down to lower mass ions and the mass spectrum becomes simpler. Eventually, at $V_{acc}=30$ V, most of the **G1** is removed from **G1** and **G3** or **G1** and **G4** combinations.[47] At low V_{acc} values, the parent ion is still intact. Upon an increase in the voltage, the smaller **G1** dissociates first and, upon a further increase in the V_{acc} value to 30 V, **G2** also dissociates. At this high V_{acc} value, some fragmentation products of **dT5** can also be seen. These CID experiments again show that **G2** binds more strongly to **dT5** than **G1**. With **G3** and **G4**, similar results were obtained.

Conclusion

We have explored the scope and limitations of ESI-MS for the detection of hydrogen-bonded supramolecular complexes of ssDNA and guest molecules. Individual ssDNA–guest complexes could be detected up to a mass of 15 kDa, which is noteworthily high since the complex consists of 20 components. CID experiments show that the hydrogen-bonded guest molecules can be dissociated from the DNA template one by one in a highly controlled way. Remarkably, we have found a linear relationship of the molecular weight of the guest molecules with the I_{50} value of the $[\mathbf{dT5{+}1\,G}x]^{3-}$ complexes, which shows that the stability is not only determined by the hydrogen-bond interaction and, therefore, a complex with a small number of guests does not necessarily retain its solution hydrogen-bonded structure in the gas phase. Interestingly, upon an increase in the collision energy of two different guests bound to **dTn** in solution, the weakest bound guest can be dissociated first. This promising tool will allow for combinatorial screening of molecules binding to DNA.

In general, we have shown that ESI-MS and CID experiments are useful techniques for identifying and studying selective and nonselective secondary interactions in templated supramolecular assemblies. These methods provide important information concerning secondary interactions in these supramolecular assemblies in the gas phase.

Experimental Section

Materials: The synthesis, purification, and characterization of **G3** and **G5** can be found in the Supporting Information. ssDNA was supplied freeze dried and HPLC purified by MWG Biotech AG. All solvents purchased from Acros Chemica, Aldrich, or Fluka were of p.a. quality. All other chemicals were commercially available and were used without further purification.

General methods: UV/Vis and fluorescence spectra were performed on a Perkin–Elmer Lambda40 and Perkin–Elmer LS-50B spectrophotometers. CD, UV/Vis, and fluorescence spectra were recorded on a JASCO 815 instrument equipped with a Peltier PFD-425S temperature controller. High-resolution ESI-MS was performed on Q-Tof Ultima Global mass spectrometer (Micromass, Manchester, UK) equipped with a Z-spray source. The analysis was performed with MassLynx 4.1 software and the spectra were deconvoluted with the MaxEnt-1 program. Electrospray ionization was achieved in the negative mode by direct and continuous injection of 0.5–4 mM solutions in MilliQ water at room temperature with a rate of 5 $\mu L\,min^{-1}$ and by applying 5 kV on the needle. The collision cell was filled with argon (1.2×10^{-3} mbar) as the collision gas and the cone voltage was set to 150 V. For a typical single-run CID experiment, the acceleration voltage was increased up to 50 V in small steps, with injection for 30 s for each V_{acc} value. From the area underneath the intensity chromatogram of the specific mass region of each ion, the relative intensities of each ion peak at every V_{acc} value could then easily be calculated.

Sample preparation: All ESI-MS samples were prepared by addition of ssDNA in MilliQ water to the solid guest and subsequent sonification of the mixture at 70 °C for at least 5 min. In the case of **G4**, a concentrated solution of **G4** in HPLC-grade tetrahydrofuran (THF) was injected into the **dT*n*** solution in MilliQ water and the THF was removed by heating the sample to 70 °C. For the titration experiments, **dT10** or **dA10** solutions were mixed with a **G1**–**dT10** (20:1) or **G1**–**dA10** (20:1) solution, respectively. Before injection into the mass spectrometer, the solutions were heated to above 70 °C to erase all memory effects and they were subsequently annealed at room temperature for at least 2 h.

Acknowledgements

The authors wish to acknowledge L. Brunsveld and M. J. Pouderoijen for supplying compounds **G2** and **G3**, respectively, K. Pieterse for the artwork, H. Eding for the elemental analysis, X. Lou for the MALDI-TOF spectra, and the EURYI scheme for financial support.

[1] H. Ihmels, D. Otto, *Top. Curr. Chem.* **2005**, *258*, 161–204.
[2] U. Pindur, M. Jansen, T. Lemster, *Curr. Med. Chem.* **2005**, *12*, 2805–2847.
[3] B. A. Armitage, *Mol. Supramol. Photochem.* **2006**, *14*, 255–287.
[4] E. J. Fechter, B. Olenyuk, P. B. Dervan, *J. Am. Chem. Soc.* **2005**, *127*, 16685–16691.
[5] K. C. Hannah, R. R. Gil, B. A. Armitage, *Biochemistry* **2005**, *44*, 15924–15929.
[6] K. C. Hannah, B. A. Armitage, *Acc. Chem. Res.* **2004**, *37*, 845–853.
[7] R. Iwaura, F. J. M. Hoeben, M. Masuda, A. P. H. J. Schenning, E. W. Meijer, T. Shimizu, *J. Am. Chem. Soc.* **2006**, *128*, 13298–13304.
[8] R. Iwaura, K. Yoshida, M. Masuda, M. Ohnishi-Kameyama, M. Yoshida, T. Shimizu, *Angew. Chem.* **2003**, *115*, 1039–1042; *Angew. Chem. Int. Ed.* **2003**, *42*, 1009–1012.
[9] R. Iwaura, M. Ohnishi-Kameyama, M. Yoshida, T. Shimizu, *Chem. Commun.* **2002**, 2658–2659.
[10] R. Iwaura, Y. Kikkawa, M. Ohnishi-Kameyama, T. Shimizu, *Org. Biomol. Chem.* **2007**, *5*, 3450–3455.
[11] P. G. A. Janssen, J. Vandenbergh, J. L. J. van Dongen, E. W. Meijer, A. P. H. J. Schenning, *J. Am. Chem. Soc.* **2007**, *129*, 6078–6079.
[12] R. F. Service, *Science* **2005**, *309*, 95.
[13] A. P. H. J. Schenning, P. Jonkheijm, F. J. M. Hoeben, J. Van Herrikhuyzen, S. C. J. Meskers, E. W. Meijer, L. M. Herz, C. Daniel, C. Silva, R. T. Phillips, R. H. Friend, D. Beljonne, A. Miura, S. De Feyter, M. Zdanowska, H. Uji-I, F. C. De Schryver, Z. Chen, F. Wuerthner, M. Mas-Torrent, D. Den Boer, M. Durkut, P. Hadley, *Synth. Met.* **2004**, *147*, 43–48.
[14] F. J. M. Hoeben, P. Jonkheijm, E. W. Meijer, A. P. H. J. Schenning, *Chem. Rev.* **2005**, *105*, 1491–1546.
[15] O. Ikkala, G. ten Brinke, *Chem. Commun.* **2004**, 2131–2137.
[16] A. Ajayaghosh, V. K. Praveen, *Acc. Chem. Res.* **2007**, *40*, 644–656.
[17] K. Tanaka, A. Tengeiji, T. Kato, N. Toyama, M. Shionoya, *Science* **2003**, *299*, 1212–1213.
[18] B. Ding, N. C. Seeman, *Science* **2006**, *314*, 1583–1585.
[19] N. C. Seeman, *Methods Mol. Biol.* **2005**, *303*, 143–166.
[20] P. W. K. Rothemund, *Nature* **2006**, *440*, 297–302.
[21] M. Brucale, G. Zuccheri, B. Samori, *Trends Biotechnol.* **2006**, *24*, 235–243.
[22] K. Lund, B. Williams, Y. Ke, Y. Liu, H. Yan, *Curr. Nanoscience* **2006**, *2*, 113–122.
[23] J. Chen, N. C. Seeman, *Nature* **1991**, *350*, 631–633.
[24] J. D. Cohen, J. P. Sadowski, P. B. Dervan, *J. Am. Chem. Soc.* **2008**, *130*, 402–403.
[25] Y. He, T. Ye, M. Su, C. Zhang, A. E. Ribbe, W. Jiang, C. Mao, *Nature* **2008**, *452*, 198–201.
[26] K. V. Gothelf, T. H. LaBean, *Org. Biomol. Chem.* **2005**, *3*, 4023–4037.
[27] J. Zhang, Y. Liu, Y. Ke, H. Yan, *Nano Lett.* **2006**, *6*, 248–251.
[28] J. H. Gross, *Mass Spectrometry: A Textbook*, Springer, Heidelberg, **2004**, p. 518.
[29] C. G. Herbert, A. W. Johnstone, *Mass Spectrometry Basics*, CRC, Boca Raton, **2002**, p. 496.
[30] I. A. Kaltashov, S. J. Eyles, *Applications of Mass Spectrometry in Biophysics: Conformation and Dynamics of Biomolecules*, Wiley, New York, **2005**, p. 368.

[31] C. A. Schalley, *Mass Spectrom. Rev.* **2002**, *21*, 253–309.
[32] C. G. Huber, H. Oberacher, *Mass Spectrom. Rev.* **2001**, *20*, 310–343.
[33] A. Apffel, J. A. Chakel, S. Fischer, K. Lichtenwalter, W. S. Hancock, *J. Chromatogr. A* **1997**, *777*, 3–21.
[34] A. Apffel, J. A. Chakel, S. Fischer, K. Lichtenwalter, W. S. Hancock, *Anal. Chem.* **1997**, *69*, 1320–1325.
[35] F. D. Lewis, L. Zhang, X. Zuo, *J. Am. Chem. Soc.* **2005**, *127*, 10002–10003.
[36] A. Cuppoletti, Y. Cho, J.-S. Park, C. Straessler, E. T. Kool, *Bioconjugate Chem.* **2005**, *16*, 528–534.
[37] M. Balaz, A. E. Holmes, M. Benedetti, P. C. Rodriguez, N. Berova, K. Nakanishi, G. Proni, *J. Am. Chem. Soc.* **2005**, *127*, 4172–4173.
[38] H. Kashida, H. Asanuma, M. Komiyama, *Angew. Chem.* **2004**, *116*, 6684–6687; *Angew. Chem. Int. Ed.* **2004**, *43*, 6522–6525.
[39] M. Rueda, F. J. Luque, M. Orozco, *J. Am. Chem. Soc.* **2006**, *128*, 3608–3619.
[40] P. G. A. Janssen, P. Jonkheijm, P. Thordarson, J. C. Gielen, P. C. M. Christianen, J. L. J. van Dongen, E. W. Meijer, A. P. H. J. Schenning, *J. Mater. Chem.* **2007**, *17*, 2654–2660.
[41] M. Elhabiri, A. Trabolsi, F. Cardinali, U. Hahn, A.-M. Albrecht-Gary, J.-F. Nierengarten, *Chem. Eur. J.* **2005**, *11*, 4793–4798.
[42] U. Hahn, M. Elhabiri, A. Trabolsi, H. Herschbach, E. Leize, A. Van Dorsselaer, A.-M. Albrecht-Gary, J.-F. Nierengarten, *Angew. Chem.* **2005**, *117*, 5472–5475; *Angew. Chem. Int. Ed.* **2005**, *44*, 5338–5341.
[43] B. J. Holliday, C. A. Mirkin, *Angew. Chem.* **2001**, *113*, 2076–2097; *Angew. Chem. Int. Ed.* **2001**, *40*, 2022–2043.
[44] F. Hof, S. L. Craig, C. Nuckolls, J. Rebek, Jr., *Angew. Chem.* **2002**, *114*, 1556–1578; *Angew. Chem. Int. Ed.* **2002**, *41*, 1488–1508.
[45] E. S. Baker, S. L. Bernstein, M. T. Bowers, *J. Am. Soc. Mass Spectrom.* **2005**, *16*, 989–997.
[46] M. A. C. Broeren, J. L. J. van Dongen, M. Pittelkow, J. B. Christensen, M. H. P. van Genderen, E. W. Meijer, *Angew. Chem.* **2004**, *116*, 3641–3646; *Angew. Chem. Int. Ed.* **2004**, *43*, 3557–3562.
[47] See the Supporting Information.
[48] J. L. Beck, M. L. Colgrave, S. F. Ralph, M. M. Sheil, *Mass Spectrom. Rev.* **2001**, *20*, 61–87.
[49] F. Rosu, V. Gabelica, C. Houssier, E. de Pauw, *Nucleic Acids Res.* **2002**, *30*, e82.
[50] F. Rosu, S. Pirotte, E. de Pauw, V. Gabelica, *Int. J. Mass Spectrom.* **2006**, *253*, 156–171.
[51] S. A. Hofstadler, R. H. Griffey, *Chem. Rev.* **2001**, *101*, 377–390.
[52] L. Brunsveld, J. A. J. M. Vekemans, J. H. K. K. Hirschberg, R. P. Sijbesma, E. W. Meijer, *Proc. Natl. Acad. Sci. USA* **2002**, *99*, 4977–4982.
[53] In the positive mode, the guest molecules can easily be detected.
[54] Note that quantitative values for guest-binding equilibrium constants cannot be obtained from these ESI-MS experiments because the free-guest concentration is not linear with the intensity of $[\mathbf{G}-\mathrm{H}]^{1-}$ and most of the complexes are partially dissociated, even at low acceleration voltages.
[55] R. D. Smith, K. J. Light-Wahl, *Biol. Mass Spectrom.* **1993**, *22*, 493–501.
[56] Note that the intensities of the peaks of the spectra in Figures 2c and 3 differ, which is presumably due to the slightly different argon pressure in the collision cell.
[57] For the original mass spectra, see the Supporting Information.
[58] With CD spectroscopy, all of the **dT*n*–G1** mixtures showed a Cotton effect in the region in which only **G1** absorbs. None of the other homo-ssDNA strands showed a Cotton effect in the **G1** absorption region. See the Supporting Information.
[59] Similar results have been obtained for **G2**, **G3**, and **G4** in combination with **dT5** and **dT20**; see the Supporting Information.
[60] The **dT20–G1** complex peaks that appeared between *m*/*z* values of 750 and 1750 Da are no longer present, which indicates that the supramolecular strand of **G1** is replaced by the **dA20** strand. Also, no complex peaks are present in the deconvoluted spectrum and it now mainly contains a **dA20** peak and a very small **dT20** peak. Although some peaks are the double-stranded **dT20–dA20** peaks, they could not be deconvoluted. It should be noted that **dT20–dA20** can polymerize into high-molecular-weight dsDNA; this makes the detection of **dT20–dA20** a lot harder.
[61] Another proof for the involvement of the amine protons in binding to the template is an experiment in which the amine protons of the diaminotriazine of **G1** were replaced with deuterium atoms by using D_2O as a solvent instead of H_2O. The mass found for the breakdown product of the **G1(D_4)–dT10** complexes corresponds to the $[\mathbf{G1(D_4)}-\mathrm{D}]^{1-}$ peak. See the Supporting Information.
[62] F. Rosu, C.-H. Nguyen, E. De Pauw, V. Gabelica, *J. Am. Soc. Mass Spectrom.* **2007**, *18*, 1052–1062.
[63] C. A. Schalley, *Analytical Methods in Supramolecular Chemistry*, **2007**, Wiley-VCH, Weinheim, p. 484.
[64] J. Gidden, A. Ferzoco, E. S. Baker, M. T. Bowers, *J. Am. Chem. Soc.* **2004**, *126*, 15132–15140.
[65] S. Sen, L. Nilsson, *J. Am. Chem. Soc.* **2001**, *123*, 7414–7422.
[66] For the same experiment with **dT5**, see the Supporting Information.

Received: July 24, 2008
Published online: November 28, 2008

